

Effect of Orientation on the Settling Characteristics of Cylindrical Particles

PAUL N. BLUMBERG and C. MICHAEL MOHR

Massachusetts Institute of Technology, Cambridge, Massachusetts

The characteristics of cylindrical particles settling in the Stokes regime in a bounded fluid are discussed. Applicable theory is reviewed and experimental data showing the effect of orientation on the terminal velocity are presented.

The settling characteristics of anisometric particles have been the subject of considerable experimental and analytical work over the past fifty years. The terminal velocity of an anisometric particle at low Reynolds number depends on orientation of the particle with respect to the gravity field, and experimental data have been gathered on cylinders and rectangular parallelepipeds (5).

It has been shown analytically that any body possessing three perpendicular planes of symmetry has no tendency to assume any particular orientation as it settles. However, anisometric particles in this category do not fall parallel to the gravity field except in certain specific orientations. This

paper deals with the settling of cylindrical particles. Applicable theory is reviewed and data showing the effect of orientation on settling velocity are presented.

UNBOUNDED FLUID

Brenner (3) has shown that for any arbitrary particle falling in Stokes' flow through an unbounded viscous fluid, the drag force on the particle is given by

$$\mathbf{f} = -6\pi\mu c (\Phi \cdot \mathbf{u}) \quad (1)$$

where c is a characteristic dimension of the particle and Φ is a symmetric resistance tensor which depends only on the geometry of the particle. Because of symmetry, Φ can be expressed in terms of three principal values associated with three orthogonal principal axes.

Paul N. Blumberg is at the University of Michigan, Ann Arbor, Michigan. C. Michael Mohr is at Arthur D. Little, Inc., Cambridge, Massachusetts.

For spheres, any orthogonal set of axes is principal axes and $\Phi = P \mathbf{I}$. The magnitude of P is unity if the radius of the sphere is selected as the characteristic particle dimension. For cylindrical particles, the principal axes are normal to the three orthogonal planes of symmetry. Therefore Φ can be expressed as

$$\Phi = i_1' i_1' \Phi_A + (i_2' i_2' + i_3' i_3') \Phi_R \quad (2)$$

where the i_j' coordinates are selected as shown in Figure 1. The principal values associated with i_2' and i_3' are equal, but different from that associated with i_1' .

In steady flow, the drag force is balanced by the gravity force on the particle, so that

$$(\Delta\rho)vg = 6\pi\mu c (\Phi \cdot \mathbf{u}) \quad (3a)$$

or

$$\mathbf{u} = \frac{(\Delta\rho)v}{6\pi\mu c} (\Phi^{-1} \cdot \mathbf{g}) \quad (3b)$$

If the gravity field and velocity vectors are expressed in the i_j coordinate system shown in Figure 1 such that $\mathbf{g} = g i_1$, the components of velocity are obtained by taking dot products of Equation (3a) with each of the unit vectors i_j and rearranging

$$u_1 = \left(\frac{(\Delta\rho)vg}{6\pi\mu c} \right) \left(\frac{\Phi_A \sin^2\theta + \Phi_R \cos^2\theta}{\Phi_A \Phi_R} \right) \quad (4a)$$

$$u_2 = \left(\frac{(\Delta\rho)vg}{6\pi\mu c} \right) \left(\frac{(\Phi_A - \Phi_R) \sin 2\theta}{2 \Phi_A \Phi_R} \right) \quad (4b)$$

$$u_3 = 0 \quad (4c)$$

Only when $\theta = 0$ or $\pi/2$ (that is, when the particle is dropped with one of its principal axes parallel to \mathbf{g}) does the particle fall parallel to \mathbf{g} . Values of Φ_A and Φ_R have been calculated only for the degenerate case of thin disks of radius c , for which (6)

$$\Phi_A = \frac{8}{3\pi} \quad (5a)$$

$$\Phi_R = \frac{16}{9\pi} \quad (5b)$$

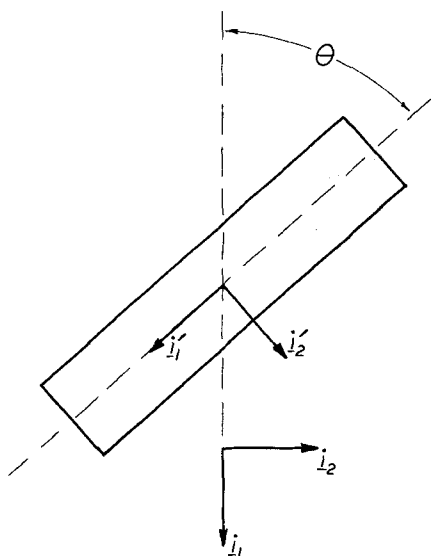


Fig. 1. Particle orientation.

WALL EFFECT

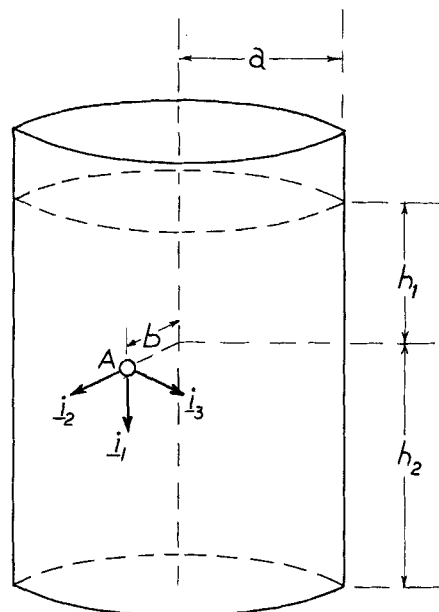


Fig. 2. Cylindrical bounding surface with particle at A.

In a bounded fluid, the steady motion of a settling particle is influenced by the containing walls. Equation (3) can be written

$$(\Delta\rho)vg = 6\pi\mu c (\phi \cdot \mathbf{u}) \quad (6a)$$

or

$$\mathbf{u} = \frac{(\Delta\rho)v}{6\pi\mu c} (\phi^{-1} \cdot \mathbf{g}) \quad (6b)$$

where the inverse of the resistance tensor ϕ^{-1} is composed of two parts (4).

$$\phi^{-1} = \left(\Phi^{-1} - \mathbf{K} \left(\frac{c}{a} \right) \right) \quad (7)$$

Φ is the resistance tensor for unbounded flow and $\mathbf{K} (c/a)$ is a wall effect term which is correct to terms of the order of (c/a) . a is a characteristic dimension of the bounding surface. \mathbf{K} is a symmetric tensor which depends on the geometry of the bounding surface and the location of the particle relative to the surface, and is independent of particle geometry. When the bounding surface consists of a cylindrical container and a free surface as shown in Figure 2, the principal axes of \mathbf{K} can be located as shown by symmetry. In general, the principal values of \mathbf{K} depend on the location of the center of the particle, denoted by b/a , h_1/a , and h_2/a . For a particle falling along the center line of the cylinder, $K_{22} = K_{33}$ and \mathbf{K} may be expressed as

$$\mathbf{K} = i_1 i_1 K_A + (i_2 i_2 + i_3 i_3) K_R \quad (8)$$

When $\mathbf{g} = g i_1$, as in Figure 1, the components of \mathbf{u} computed from Equation (6b) are

$$u_j = \left(\frac{\Delta \rho v g}{6\pi \mu c} \right) \Phi_{j,1}^{-1} \quad (9)$$

where

$$\Phi_{j,1}^{-1} = i_j \cdot \Phi^{-1} \cdot i_1 \quad (10)$$

Evaluation of $\Phi_{j,1}^{-1}$ from Equation (7) yields

$$u_1 = \frac{(\Delta \rho) v g}{6\pi \mu c} \left(\frac{\Phi_A \sin^2 \theta + \Phi_R \cos^2 \theta}{\Phi_A \Phi_R} - K_A \left(\frac{c}{a} \right) \right) \quad (11a)$$

$$u_2 = \frac{(\Delta \rho) v g}{6\pi \mu c} \left(\frac{(\Phi_A - \Phi_R) \sin 2\theta}{2 \Phi_A \Phi_R} \right) \quad (11b)$$

$$u_3 = 0 \quad (11c)$$

Note that the wall effect on u_1 is independent of particle orientation, relative to the gravity field.

Rearrangement of Equation (11a) yields

$$\hat{u} = \frac{u_1}{\left(\frac{(\Delta \rho) v g}{6\pi \mu c} \right)} = \left(\frac{1}{\Phi_R} - \frac{1}{\Phi_A} \right) \sin^2 \theta + \left(\frac{1}{\Phi_A} - K_A \left(\frac{c}{a} \right) \right) \quad (12)$$

The principal values Φ_A and Φ_R can be obtained directly from experimental measurements of \hat{u} at $\theta = 0$ and $\pi/2$, or alternatively by regression techniques from a series of measurements distributed over θ .

If the characteristic dimension of the particle is taken to be the radius of a sphere of equal volume, \hat{u} is the ratio of the terminal velocity of the particle as measured to that of an equal-volume sphere in an unbounded fluid.

To correct experimental data for wall effect, the value of K_A must be known. The value of K_A depends on the position of the particle with respect to the upper fluid-air interface and the bottom of the container. However, Brenner (2) showed that the theoretical value of K_A applying to an infinite cylindrical container ($h_1/a \gg 1$, $h_2/a \gg 1$) fit the data of Heiss and Coull (5) taken in a finite cylinder. From the description of the apparatus used, it is estimated that h_1/a and h_2/a varied from approximately 3.5 to 10.5 during the settling of a particle. Over this range of variation, K_A appears to be nearly independent of h_1/a and h_2/a . A similar comparison with the data on isometric particles presented by Pettyjohn and Christiansen (7) bore out this conclusion.

APPARATUS AND PROCEDURE

The cylindrical particles used were fabricated from 0.25-in. cylindrical aluminum stock, taking care to produce symmetrical cylinders. Eight sizes were used, ranging in diameter from 0.096 to 0.312 cm., in length from 0.096 to 0.275 cm., and in h/d from 0.31 to 2.86. The density of the stock was measured to be 2.7850 ± 0.005 g./cc.

The fluid used was Ucon-HB-5100, a mixture of polyalkene glycols and their derivatives. After equilibration with ambient laboratory conditions, the density of the fluid was measured to be 1.047 ± 0.005 g./cc. and found to be essentially constant over the temperature range of interest (19° to $23^\circ\text{C}.$). The fluid viscosity (of the order of 25 poise) was measured frequently during the course of the settling experiments by the falling sphere method with a steel ball-bearing 0.2380 cm. in diameter.

The particles were settled in a cylindrical glass tank 14.2 cm. in inner diameter and approximately 46 cm. in height. Timing rings were marked on the cylinder, the lower ring being approximately 10 cm. from the bottom of the tank and the upper ring being 25.4 cm. above the lower. Vertical lines

were marked over one quadrant of the cylinder to facilitate determination of particle orientation.

Terminal velocities were measured by timing the fall of the particles between the two horizontal rings on the tank with an H. C. Thompson sweeptimer graduated in 0.2-sec. divisions. Orientations of the particles were measured to $\pm 2^\circ$ with a two-lens magnifying system. A hairline on one lens was aligned with the vertical tank markings, while a hairline on the other (moveable) lens was oriented along the particle axis.

Initial tests showed that the fluid viscosity varied less than 0.1 poise/20-min. period over the range of ambient conditions encountered in the laboratory. Timing the fall of a particle over several portions of the 25.4-cm. measurement zone showed no measureable effect of the proximity of the upper and lower fluid surfaces to the marking rings delineating the measurement zone.

In separate trials, each particle was released beneath the fluid surface from tweezers and the orientation of the particle was adjusted with a thin steel rod immediately after release. In falling through the 10 cm. of fluid above the upper marking ring, the particle reached terminal velocity and any immersion disturbances were dissipated. A viscosity measurement was made every 15 to 20 min. during experimentation; at no time was more than one particle falling through the fluid.

The values of \hat{u} computed from the measured time intervals and fluid properties were estimated to have a maximum error of approximately 1.5%, equally divided among timing the fall of the cylindrical particles, timing the fall of the sphere in the viscosity measurements and possible variation in viscosity between measurements. Estimates of error computed from limited replicated data agreed with the 1.5% value.

RESULTS

Terminal velocities were measured for the eight particles ranging from 0.31 to 2.86 in h/d as a function of orientation. Principal values of Φ were determined by least-squares fitting of Equation (12) to each set of data. The infinite-cylinder wall-effect factor $K_A = 2.104$ was used, neglecting the effects of variation in distances to the top and bottom of the tank and slight deviations of the particles from the centerline of the tank which are accentuated by the lateral drift of the particles at orientations other than $\theta = 0$ or $\pi/2$. Maximum lateral displacement of the cylinders due to drift amounted to approximately 0.5 cm. and the error in initial placement of the particle did not amount to more than 0.5 cm. From values given by Brenner (2) the change in K_A associated with a 1-cm. displacement from the centerline is approximately -0.1 , a negligible difference.

Heiss and Coull (5) presented data on the terminal velocities of cylinders in the two orientations $\theta = 0$, $\pi/2$. For these special orientations Equation (12) reduces to

$$\hat{u}_0 = \frac{1}{\Phi_A} - K_A \left(\frac{c}{a} \right) \quad (13a)$$

$$\hat{u}_{90} = \frac{1}{\Phi_R} - K_A \left(\frac{c}{a} \right) \quad (13b)$$

Plots of measured values of \hat{u}_0 and \hat{u}_{90} vs. d were extrapolated to $d = 0$ to give the principal values Φ_A and Φ_R . As indicated previously the slopes of their plots agree within experimental error with the slopes predicted using $K_A = 2.104$ and the geometric properties of the system used.

Principal value data for both studies are shown in Figure 3. There is good agreement, except at low and high (h/d). The discrepancy is probably due to imperfections in the particles used.

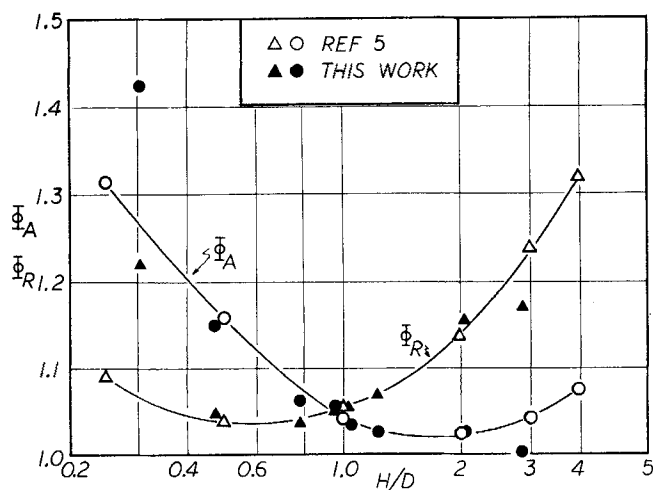


Fig. 3. Principal values of resistance tensor.

The data on effect of orientation at intermediate values of θ can be presented in a normalized form. It is evident from Equation (12) that \hat{u}_0 and \hat{u}_{90} are extreme values of \hat{u} . Measured values of \hat{u} obtained with different particles can be put on a common basis by defining a normalized terminal velocity:

$$\psi = \frac{\hat{u} - \hat{u}_{\min}}{\hat{u}_{\max} - \hat{u}_{\min}} \quad (14)$$

Combination of Equations (12) and (13) yields

$$\psi = \sin^2 \beta \quad (15)$$

where

$$\begin{aligned} \beta &= \theta & \hat{u}_0 < \hat{u}_{90} \\ \beta &= \pi/2 - \theta & \hat{u}_0 > \hat{u}_{90} \end{aligned}$$

The data for four of the particles tested are shown in Figure 4 along with the theoretical curve $\psi = \sin^2 \beta$. Approximate σ limits of error are shown for each particle. Data for particles with h/d near to unity are not included since the experimental error was excessive relative to the maximum change in velocity with orientation. The data fit the theoretical curve reasonably well in light of the experimental error present.

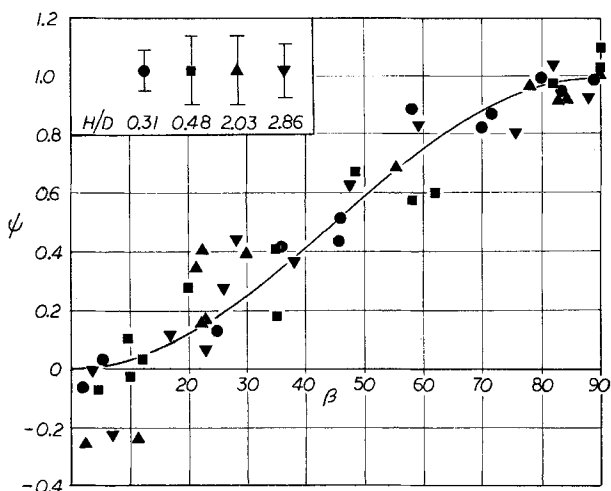


Fig. 4. Effect of orientation on terminal velocity.

SUMMARY

The settling behavior of anisometric particles can be predicted for all orientations of the particle relative to the gravity field from the three principal values of the resistance tensor. For the cylindrical particles studied, the measured terminal velocities agree with those predicted within the experimental error present.

ACKNOWLEDGMENT

Thanks are expressed to the Union Carbide Corporation for the Ucon fluid used in the experiments.

NOTATION

- a = characteristic dimension of boundary surface, cm.
- b = distance from center of particle to center line of boundary cylinder, cm.
- c = characteristic dimension of particle, cm.
- d = diameter of cylindrical particle, cm.
- f, \mathbf{f} = drag force exerted on settling particle, dynes
- g, \mathbf{g} = acceleration of gravity, 980.7 cm./sec.²
- h = length of cylindrical particle, cm.
- h_1 = distance from center of particle to upper boundary surface
- h_2 = distance from center particle to lower boundary surface
- \mathbf{I} = identity tensor, dimensionless
- \mathbf{K} = wall effect tensor, dimensionless
- K_{ij} = component of wall effect tensor, dimensionless
- u, \mathbf{u} = particle velocity, cm./sec.
- \hat{u} = dimensionless terminal velocity [see Equation (12)]
- v = particle volume, cc.

Greek Letters

- β = angle related to orientation of particle [see Equation (15)]
- θ = orientation of particle (see Figure 1)
- μ = viscosity, poise
- ρ = density, g./cc.
- Φ = resistance tensor in an infinite fluid, dimensionless
- ϕ = resistance tensor in a bounded fluid, dimensionless
- Φ_{ij} = components of resistance tensor in infinite fluid, dimensionless
- ϕ_{ij} = components of resistance tensor in bounded fluid, dimensionless
- ψ = normalized dimensionless terminal velocity [see Equation (14)]

LITERATURE CITED

1. Blumberg, Paul, S. B. thesis, Massachusetts Inst. Technol., Cambridge (1965).
2. Brenner, Howard, *J. Fluid Mech.*, **12**, 35-48 (1962).
3. ———, *Chem. Eng. Sci.*, **18**, 1-25 (1963).
4. ———, *J. Fluid Mech.*, **18**, 144-158 (1964).
5. Heiss, J. F., and J. Coull, *Chem. Eng. Progr.*, **48**, 133-140 (1952).
6. Landau, L. D., and E. M. Lifshitz "Fluid Mechanics," p. 67, Addison-Wesley, Reading Mass. (1959).
7. Pettyjohn, E. S., and E. B. Christiansen, *Chem. Eng. Progr.*, **44**, 171 (1948).

Manuscript received November 16, 1966; revision received June 6, 1967; paper accepted June 9, 1967.